Performance Comparison among Multicrystalline Silicon, Anti-Reflective Coated and Bare Cadmium Telluride Photovoltaic Technologies in Southern Brazil

Marília Braga[1], Anelise Medeiros Pires[2], Clarissa Debiazi Zomer[1] and Ricardo Rüther[1]

[1] Universidade Federal de Santa Catarina-UFSC, Florianópolis (Brazil)

[2] IESS IDEAL Estudos e Soluções Solares, Florianópolis (Brazil)

Abstract

This study aims to analyze the performance of mc-Si, bare and antireflective-coated (ARC) CdTe photovoltaic (PV) modules in Florianópolis, Brazil (27°S, 48°W). Results obtained from data for the full year of 2018 revealed that both bare and ARC-coated CdTe systems are great performers at the local operating conditions, with PR values 2.1% and 5.8% higher than those obtained for mc-Si, respectively. This can be explained by local high temperatures and a blue-shifted solar spectrum, both characteristics favoring low-temperature-coefficient and blue-biased thin-film CdTe. For winter months, when the local spectrum is redder and temperatures are lower, mc-Si performed slightly better. Comparison between bare and ARC CdTe reveals that ARC had a 3.6% higher PR value over bare CdTe modules for the year, winter months being the time of the year that favors the most the use of this coating, due to this period's higher incidence angles.

Keywords: PV systems; performance analysis; CdTe; crystalline silicon; anti-reflective coating; ARC; spectrum.

1. Introduction

While traditional silicon technologies dominate the scene, with some 97% of the world market in 2018 (Mints, 2018), high-efficiency and large-area, new generation thin-film cadmium telluride (CdTe) PV modules have recently been introduced in the market with record-breaking efficiencies (Strevel, 2017). The lower temperature coefficient on power, and the blue-shifted spectral response when compared to multicrystalline silicon (mc-Si), render thin-film CdTe good performers in the warm, sunny, humid and bluer skies predominant in sunbelt regions of the world (Munshi et al., 2018). This study aims to analyze the monthly and annual performance of three fixed-tilt, North-oriented PV systems in Florianópolis, Brazil (27°S, 48°W), installed at the Fotovoltaica-UFSC solar research laboratory. The first system is based on mc-Si PV modules; the second, on CdTe; and the third, on CdTe with anti-reflexive coating (ARC).

Campos et al. (2018) and do Nascimento et al. (2020, 2018, 2016), among others, have reported in the literature a performance advantage for CdTe over mc-Si in Brazilian warm and sunny climates. This performance advantage can be attributed to this technology's lower temperature coefficient on power and blue-shifted spectral response (Braga et al., 2019a, 2019b). Furthermore, anti-reflective coated CdTe aims at introducing an even larger advantage to these PV modules, by reducing the incidence angle losses (IAM) at normal incidence - increasing CdTe's nameplate power - and at other angles as well, leading to better performance in real operating conditions (Grammatico e Littmann, 2018; Passow et al., 2018).

By comparing the performance of real life PV systems, this study aims at further investigating such advantages of CdTe and ARC CdTe over traditional mc-Si for warm and sunny climates. No such comparison between these three types of PV modules has been done for the Brazilian climate, which is a relevant market for the PV industry, with great solar resource (Pereira et al., 2017) and a rapidly growing PV installed capacity (Lopes, 2017; PV Magazine Latin America, n.d.).

© 2019. The Authors. Published by International Solar Energy Society
Selection and/or peer review under responsibility of Scientific Committee
doi:10.18086/swc.2019.14.02 Available at http://proceedings.ises.org

2. Experimental Setup and Methodology

To evaluate the performance of bare CdTe, ARC-coated CdTe, and mc-Si PV technologies in Southern Brazil, data from three ground-mounted PV systems installed in Florianópolis-SC (27°S, 48°W), as shown in Fig. 1, were collected, filtered and analyzed for the full year of 2018. The main electrical characteristics of the PV systems used in this study, as well as their orientation and tilt, are shown in Tab. 1. The systems were designed to have the best matching characteristics possible, in order to reduce the uncertainties and variables affecting the performance comparison among the PV technologies. Each system is connected to a 2.5 kW isolated string inverter; all three systems have identical inverters.

Electrical parameters measurements were acquired with a one-minute resolution from each of the PV systems' inverters by a Campbell CR6 datalogger. DC data were preferred over AC because the actual power output of the different PV technologies was the target of this analysis, not the overall performance of the systems.

Tab. 1: Main electrical and layout characteristics of the PV systems used in this study[1].

Parameter	mc-Si	CdTe	CdTe w/ ARC
Nominal Module Power	235 W_p	110 W_p	110 W_p
Module Efficiency	14.2%	15.3%	15.3%
Modules in Series	10	5	5
Strings in Parallel	1	4	4
String Open Circuit Voltage	368 V	436 V	436 V
Total System Peak Power	2.35 kW_p	2.2 kW_p	2.2 kW_p
Inverter Nominal Power	2.5 kW	2.5 kW	2.5 kW
Total System Area	16.5 m^2	14.4 m^2	14.4 m^2
Azimuth Angle	0°	0°	0°
Tilt Angle	20°	18°	16°

Fig. 1: Aerial view of the three PV systems located at the Fotovoltaica-UFSC research laboratory in Florianópolis, Brazil (27°S, 48°W) and used in the present study (mc-Si, CdTe and CdTe with ARC)

Global and diffuse horizontal irradiance (GHI and DHI) data with a one-minute resolution were also acquired from a Delta SPN1 pyranometer installed at the local weather station, shown in Fig. 2 and described in Tab. 2. These data were then transposed to obtain the global plane of array irradiance (G_{POA}) for the PV systems under study using the PVsyst V6.74 simulation software. Other environmental data were also acquired from various sensors installed at the same weather station shown in Fig. 2, such as ambient temperature, relative humidity, rainfall and wind speed.

[1] All values are given for Standard Test Conditions (STC): 1000 W/m^2 irradiance, 25°C cell temperature and AM1.5G spectrum, according to EN 60904-3.

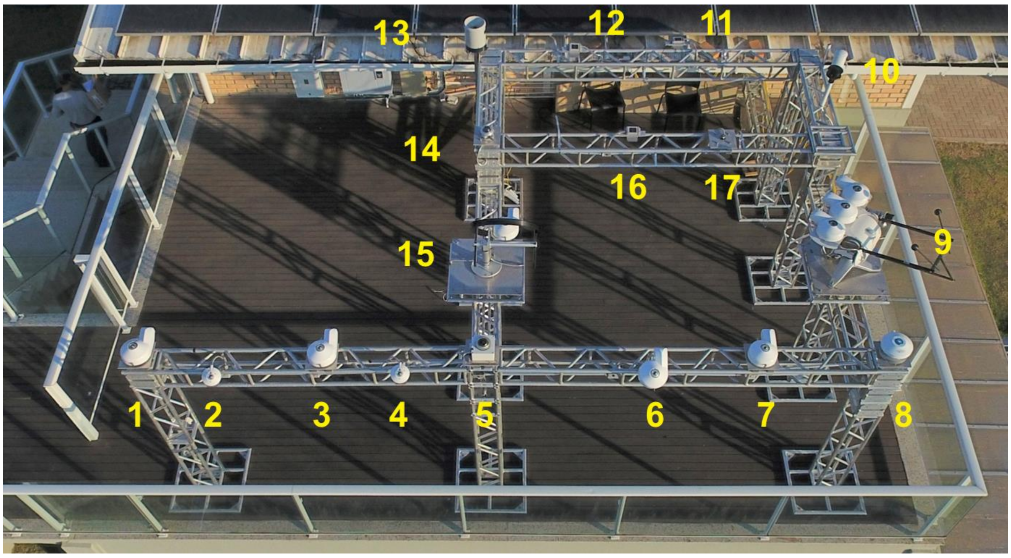

Fig. 2: Aerial view of the solar measurement station located at the Fotovoltaica-UFSC research laboratory in Florianópolis, Brazil (27°S, 48°W), numbered according to Tab. 2, from where solar and environmental data were obtained for the present study.

Tab. 2: List of sensors installed at the Fotovoltaica-UFSC research laboratory in Florianópolis, Brazil (27°S, 48°W), numbered according to Fig. 2.

Sensor #	Measurement	Model	Manufacturer
1	*Ultraviolet*	*CUV-5-V*	*Kipp & Zonen*
2	*Global Tilted Irradiance*	*SMP6*	*Kipp & Zonen*
3	*Global Horizontal Irradiance*	*SMP11-V*	*Kipp & Zonen*
4	*Global Tilted Irradiance*	*SMP11*	*Kipp & Zonen*
5	*All- Sky Camera*	*SRF-02*	*EKO*
6	*Global Tilted Irradiance*	*SMP11-V*	*Kipp & Zonen*
7	*Global Horizontal Irradiance*	*SMP22-V*	*Kipp & Zonen*
8	*Solar Spectrum*	*MS-711*	*EKO*
9a	*Infrared & Long-Wave*	*SGR4-V*	*Kipp & Zonen*
9b	*Global Horizontal Irradiance*	*SMP22-V*	*Kipp & Zonen*
9c	*Diffuse Horizontal Irradiance*	*SMP22-V*	*Kipp & Zonen*
9d	*Direct Normal Irradiance*	*SHP1-V*	*Kipp & Zonen*
9e	*Global Tilted Irradiance (1-Axis)*	*SMP11-V*	*Kipp & Zonen*
9f	*Global Tilted Irradiance (2-Axis)*	*SMP11-V*	*Kipp & Zonen*
10a	*Wind Speed and Direction*	*WINDSONIC1*	*GILL*
10b	*Relative Humidity & Temperature*	*HMP155A*	*VAISALA*
11	*Global Horizontal Irradiance*	*Si-02-PT100*	*IMT*
12	*Global Tilted Irradiance (Clean)*	*Si-02-PT100*	*IMT*
13	*Pluviometer*	*TB4-L*	*HS*
14	*Global/Diffuse Horizontal Irradiance*	*SPN1*	*Delta-T*
15	*Diffuse Horizontal Irradiance*	*SMP11*	*Kipp & Zonen*
16	*Global Tilted Irradiance (Soiled)*	*Si-02-PT100*	*IMT*
17	*Photosynthetically Active Radiation (PAR)*	*PQS-1*	*Kipp & Zonen*

PVsyst offers its users two options as far as transposition models go: Hay's model (Hay, 1979) and the Perez-Ineichen model (Perez et al., 1990). The two models differ only in the way they transpose the diffuse component of radiation. Hay's model divides the diffuse component into isotropic and circumsolar, while the Perez-Ineichen model introduces a third component: the horizon band. PVsyst describes the Hay model as classic and robust, and used this model as its default transposition model up to the version 5 of the software. However, recent findings showed that the Perez-Ineichen yields better results in any case (Ineichen, 2011), therefore recent versions of the software now use this model by default and this was the model chosen to transpose irradiance data in the present study. The maximum possible time resolution for data computation in PVsyst is one-hour, therefore, all other data were integrated into one-hour averages in order to use the transposed irradiance data.

Due to nearby buildings and a wind turbine (visible on Fig. 1), parts of the analyzed systems are subject to shading during certain times of the day and year. Annual shadings were quantified using the shading masks computed by the Ecotect software, as described in Zomer and Rüther (2017) and shown in Fig. 3. The presence of the above-mentioned buildings west of all three systems and the wind turbine east of the mc-Si and south/southeast of the CdTe systems can be observed on the shading masks. In this shading study, all points of the PV systems were analyzed, with darker areas in the shading masks being a result of obstacles that affect a big portion of the system, while lighter grey areas are objects that only obstruct the PV system under study partially. Overall, the analysis resulted in 9.7% of annual shading for mc-Si, 11% for bare CdTe and 8% for ARC-coated CdTe.

Fig. 4 shows the hourly shading patterns from 9:00 until 17:00 for the three analyzed PV systems: mc-Si (grey), CdTe (orange) and CdTe with ARC (blue) for June (Fig. 4a) and December (Fig. 4b). It is clear that shading affects more strongly the PV systems during the winter months, when the sun is lower in the sky.

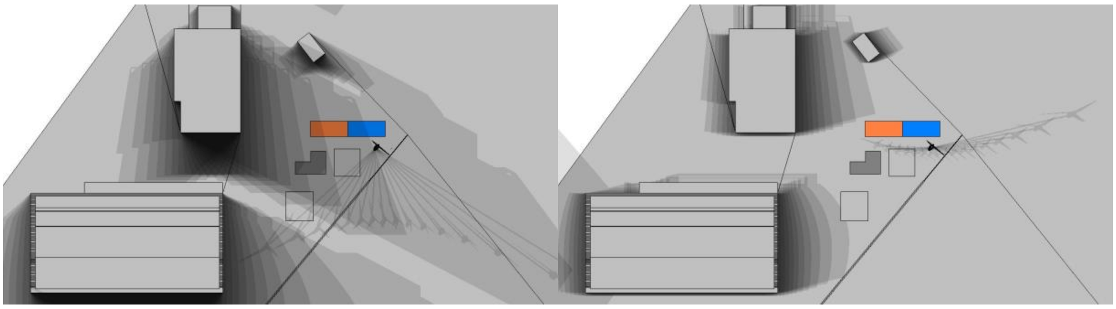

(a) (b)

Fig. 4: Ecotect shading patterns for June (a) and December (b) obtained from Ecotect for the analyzed PV systems: mc-Si (grey), bare CdTe (orange) and CdTe with ARC (blue).

Fig. 5 shows the results from Fig. 4 translated into percentage of shading for each of the three systems in an hourly basis for a full year. Based on this, it was decided to consider for the analysis only the time period from 9:00 until 16:00, period in which shading of the systems is minimum during all times of the year. It is important to highlight that the two PV technologies under study have very distinct behaviors when submitted to partial shading: while mc-Si modules are divided in substrings by bypass diodes, CdTe modules present a linear shading loss.

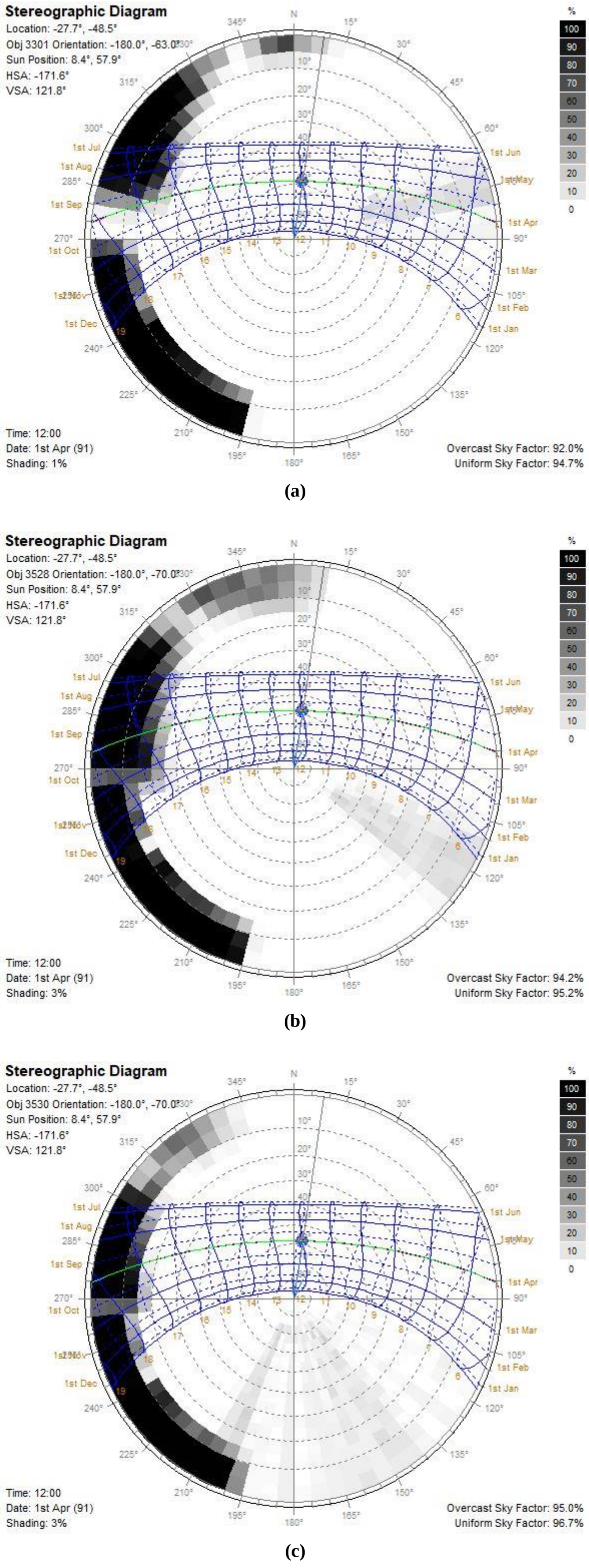

Fig. 3: Ecotect shading masks used in the shading analysis of the systems under study: mc-Si (a); bare CdTe (b) and CdTe with ARC (c).

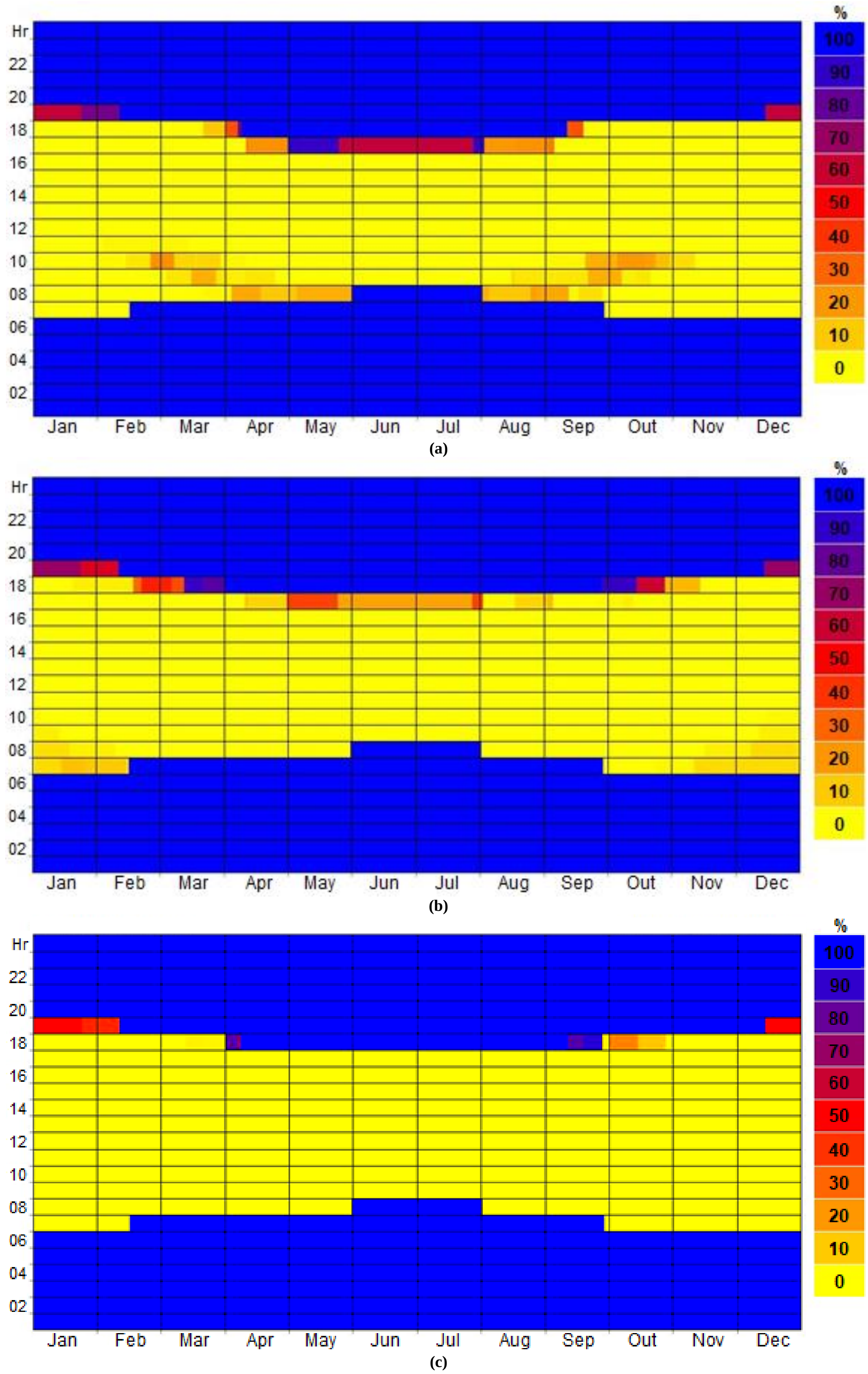

Fig. 5: Shading patterns obtained from Ecotect for all three PV systems used in this study: mc-Si (a); bare CdTe (b) and CdTe with ARC (c).

Data from all the PV systems and the pyranometer were also individually filtered for invalid values, then cross-checked, and only data points where all PV systems were operating simultaneously and there were irradiance data available were used. As mentioned above, one-minute data were grouped into hourly averages, and only hours with more than 30 data points (30 minutes) were considered valid. Hourly data were then integrated into daily values and only days with more than 6 valid hours were taken into account. Daily values were then integrated into monthly energy and irradiation values and only months with more than half of the days were considered well-founded. Data from incomplete months that met the aforementioned criteria were extrapolated to obtain a value representative for a full month of data.

From monthly energy and irradiation data, figures of merit, such as yield and performance ratio (PR), were calculated in order to characterize the performance of the PV systems under study. The yield of a PV system ($Yield$) relates the energy output of a PV system (E, given in kWh) with its installed nominal peak power (P_{STC}, given in kW_p), as shown in eq. (1). Given that the systems under study are subject to nearly the same irradiation and environmental conditions, the yield is a valid comparison metric.

$$Yield = \frac{E}{P_{STC}} \qquad \text{(eq. 1)}$$

To better evaluate systems operating under different conditions (i.e. different locations and/or orientation and tilt angles), the performance ratio is a better-suited metric because it also takes into consideration the plane of array (POA) irradiation. Considering the slightly different tilt of the analyzed systems, the performance ratio of the systems under study was also calculated using measured global and diffuse irradiance transposed for each of the systems' tilt angles (see Tab. 1) as explained above. The equation used for PR calculation is shown in eq. (2). H_{POA} represents the total plane of array global irradiation for the analyzed period, given in kWh/m^2, given in ; E is the total energy generated in the analyzed period, given in kWh; G is the reference irradiance, which equals to 1 kW/m^2; and P_{STC} is the total nominal power of the system, given in kW_p.

$$PR = \frac{E \times G}{H_{POA} \times P_{STC}} \qquad \text{(eq. 2)}$$

3. Results and Discussion

Tab. 3 presents the total number of valid days in each of the months considered in this analysis. May/18 is the only month that did not meet the minimum criteria to be considered a valid month in this study. Overall, 70% of the total days in 2018 were valid for this study. The main problem with data used in this study was caused by communication faults in the data acquisition setup for the PV systems, leading to data gaps.

Tab. 3: Number of valid days for the months considered in the analysis. May/18 is the only month with less than 50% of valid days, and therefore results for this month should be disregarded.

Month	Total	Actual	Fraction
Jan/18	31	18	58%
Feb/18	28	25	89%
Mar/18	31	26	84%
Apr/18	30	21	70%
May/18*	31	10	32%
June/18	30	18	60%
July/18	31	26	84%
Aug/18	31	27	87%
Sept/18	30	23	77%
Oct/18	31	22	71%
Nov/18	30	21	70%
Dec/18	31	19	61%
Annual	365	256	70%

Fig. 6 shows the monthly yield results for all three PV technologies under study: mc-Si (grey bars), bare CdTe (orange bars) and ARC-coated CdTe (yellow bars). Average monthly global POA irradiation for all systems (solid green line) and average ambient temperature (dotted blue line) are also shown. A seasonal fluctuation of yield values due to natural solar resource variation can be observed, with higher irradiation - and thus yield values - for the summer months. Yield results are not comparable to those previously found for the same region due to data filtering for moments at which the PV systems experience shading from nearby buildings and/or wind turbine.

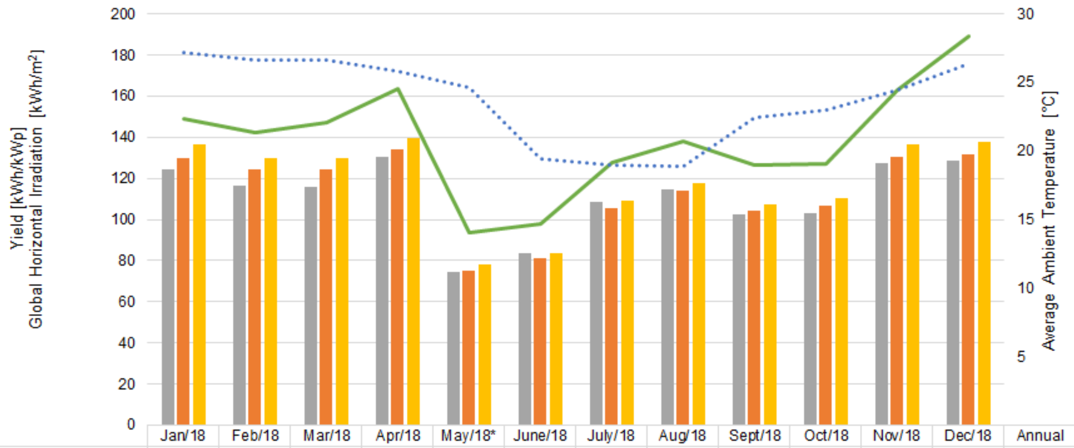

	Jan/18	Feb/18	Mar/18	Apr/18	May/18*	June/18	July/18	Aug/18	Sept/18	Oct/18	Nov/18	Dec/18	Annual
Yield mc-Si	124	116	116	130	75	84	109	115	102	103	127	128	1329
Yield CdTe	130	124	124	134	75	81	106	114	104	106	131	132	1362
Yield ARC CdTe	137	130	130	140	78	84	109	118	107	110	137	138	1416
HPOA [kWh/m2]	149	142	147	164	94	98	128	138	127	127	163	189	1666
Ambient Temp. [°C]	27	27	27	26	25	19	19	19	22	23	24	26	24

Fig. 6: Measured monthly yield (kWh/kW$_p$) during the analyzed period (2018) for the three PV systems under study: mc-Si (grey bars), bare CdTe (orange bars) and ARC-coated CdTe (yellow bars). Data were filtered in order to minimize shading from nearby objects and buildings. Monthly global tilted irradiation (solid green line) and average ambient temperature (dotted blue line) are also shown.

It can be observed that, overall, ARC-coated CdTe has the best performance throughout the year, with an annual yield of 1416 kWh/kW$_p$, 6% higher than the annual yield found for the traditional and market-dominant mc-Si (1329 kWh/kW$_p$). CdTe presented an annual yield of 1362 kWh/kW$_p$, 2% higher than mc-Si. These results are particularly important considering that mc-Si is the best oriented system (20° tilt at a 27° latitude site), while CdTe with ARC is the worst oriented system (16° tilt).

PR calculated from transposed irradiance data and DC measured power for all three systems under study is shown in Fig. 7. PR for mc-Si is represented by a grey line with triangular markers, PR for bare CdTe is represented by an orange line with square markers, and for CdTe with ARC, PR is represented by a yellow line with diamond markers. The monthly irradiance-weighted ambient temperature is also shown as blue bars.

The better performance of thin-film CdTe can be attributed to this technology's blue-shifted spectral response - that matches more closely the local blue-biased spectrum - and its low temperature coefficient on power (-0.34%/°C *vs.* -0.45%/°C for mc-Si), a great advantage on the local humid subtropical climate (Cfa, according to Köppen-Geiger's climate classification (Alvares et al., 2013)).

Nevertheless, it can also be observed that mc-Si performs better during months surrounding the Southern Hemisphere's winter solstice (June 21st). This can be explained by the higher air mass values, resulting in greater air mass (AM) values for this time of the year, culminating in a redder solar spectrum, which in turn favors low-band-gap PV technologies such as mc-Si. Furthermore, the low temperature coefficient advantage that CdTe has over mc-Si in this region is not as relevant during the winter months, period in which the ambient temperature averaged only about 20°C on the evaluated year.

PR differences between CdTe with ARC and mc-Si ranged from 9.7% in March to 2.9% in June. Non-ARC CdTe presented a similar variation when compared to mc-Si, with a maximum PR 5.8% higher than mc-Si in March and a minimum of -1.2% in June. When comparing ARC and non-ARC CdTe, results show that modules with ARC have a year-round superior performance (3.6% on average), with a more prominent advantage in

April, with 4.4% higher performance ratio results. These results corroborate previous findings from similar studies (Passow et al., 2018; Perers et al., 2015).

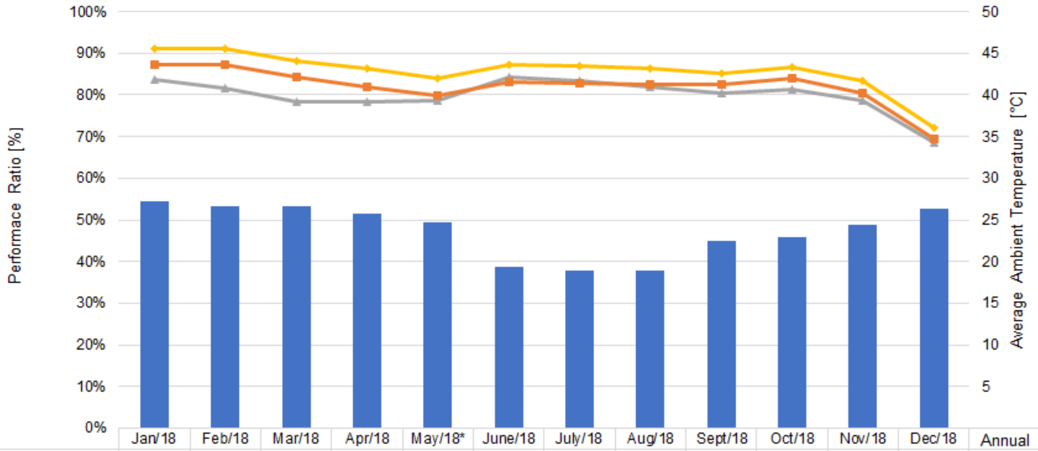

	Jan/18	Feb/18	Mar/18	Apr/18	May/18*	June/18	July/18	Aug/18	Sept/18	Oct/18	Nov/18	Dec/18	Annual
Ambient Temp. [°C]	27	27	27	26	25	19	19	19	22	23	24	26	24
PR mc-Si	84%	82%	78%	78%	79%	84%	83%	82%	80%	81%	79%	68%	80%
PR CdTe	87%	87%	84%	82%	80%	83%	83%	82%	82%	84%	80%	70%	82%
PR ARC CdTe	91%	91%	88%	86%	84%	87%	87%	86%	85%	87%	83%	72%	86%

Fig. 7: Calculated monthly PR (%) during the analyzed period (2018) for the three PV systems under study: mc-Si (grey line with triangles), CdTe (orange line with squares) and ARC-coated CdTe (yellow line with diamonds). Data were filtered in order to minimize shading from nearby objects and buildings. Monthly average ambient temperature (blue bars) are also shown.

The purpose of ARC coating is to minimize IAM losses caused by non-normal incidence of light on the surface of PV modules. These IAM losses are greater in the mornings and late afternoons, due to the Sun's trajectory throughout the day. In the case of the analyzed PV systems, IAM losses are also greater during winter months due to the low tilt angles of the systems and the Sun being lower in the sky during this time of the year, resulting in a more oblique incidence of light on the panel's surface. Even with the filtering of early morning and late afternoon data (time periods where partial shading was affecting one or more systems), times at which ARC-coated CdTe would have great advantage over non-ARC CdTe; the anti-reflexive coating still presented great advantage on the monthly PR and yield results.

4. Conclusions

Results showed that new generation thin-film CdTe has great performance advantages (up to almost 10%) over traditional mc-Si on humid subtropical climates such as the one found in Florianópolis, especially during summer months, due to its low temperature coefficient and blue-shifted spectral response, as previously presented by Braga et al. (2019a).

Even though it is the least well oriented out of the analyzed systems, ARC-coated CdTe showed the best overall annual yield (1416 kWh/kW$_p$), followed by bare CdTe (1362 kWh/kW$_p$) and mc-Si (1329 kWh/kW$_p$). Absolute yield values should not be compared to previous results for the region due to the use of the aforementioned data filtering process that excludes several hours of day from the analysis due to partial shading effects affecting one or more of the PV arrays analyzed in this work. Yield values presented a natural seasonality, due to the local solar resource having a seasonal behavior. Some of the PV technologies' characteristics also add a component to the yearly profile of the monthly yield values, such as spectral responsivity and IAM characteristics.

Annual average PR values were 79.9%, 82.1% and 85.7% for mc-Si, bare CdTe and CdTe with ARC, respectively. ARC-coated CdTe presented a 3.7% annual higher performance ratio than bare CdTe, with winter months being the months with the highest gains for ARC-coated CdTe over bare CdTe (reaching up to 4.2% differences). This seasonality can be attributed to higher incidence angles during the winter months, accentuating the performance advantage of the ARC-coated technology when it comes to angle of light incidence. It is important to highlight that this analysis is conservative, as times of the day where significant shading in any of the systems is present were disregarded, leaving out parts of the day in which ARC-coated

CdTe would theoretically perform better than bare CdTe (early morning and end of afternoons). Silicon PV modules also presented a slight increase in PR during the winter months, caused by higher air mass values and lower precipitable water content in the atmosphere, resulting in a redder spectral distribution of light, which in turn benefits this low band gap PV technology.

5. Further Work

Further investigations should be done using shading corrected irradiance data to avoid leaving out periods in which ARC-coated might have great advantage over bare CdTe. A comparison between expected and actual energy yield and performance of the PV systems is also advised, using a 3D model to simulate shading from the nearby buildings and wind turbine.

Back-of-module temperature measurements should be considered in the future to better quantify the low temperature coefficient advantage of CdTe over mc-Si and assess the accuracy of back-of-module temperature estimation models in such PV technologies, mounting type and climatic conditions.

Finally, a spectral analysis shall be conducted to better quantify spectral gains of CdTe over mc-Si for the given location. These spectral calculations can be done either with measured spectral data from the above-mentioned solar measurement station, or with empirical direct methods using environmental parameters as inputs.

References

Alvares, C.A., Stape, J.L., Sentelhas, P.C., De Moraes Gonçalves, J.L., Sparovek, G., 2013. Köppen's climate classification map for Brazil. Meteorol. Zeitschrift 22, 711–728. https://doi.org/10.1127/0941-2948/2013/0507

Braga, M., Nascimento, L.R. do, Rüther, R., 2019a. Spectral modeling and spectral impacts on the performance of mc-Si and new generation CdTe photovoltaics in warm and sunny climates. Sol. Energy 188, 976–988. https://doi.org/10.1016/j.solener.2019.06.073

Braga, M., Nascimento, L.R. do, Rüther, R., 2019b. Spectral Impacts on the Performance of mc-Si and New-Generation CdTe Photovoltaics in the Brazilian Northeast, in: Proceedings of the 46h IEEE Photovoltaic Specialists Conference. Chicago, USA.

Campos, R.A., do Nascimento, L.R., Braga, M., Simões, G., Rüther, R., 2018. Performance Assessment of PV Technologies and Complementarity of Utility-Scale PV and Wind Power Plants in Brazil, in: 2018 IEEE 7th World Conference on Photovoltaic Energy Conversion, WCPEC 2018 - A Joint Conference of 45th IEEE PVSC, 28th PVSEC and 34th EU PVSEC. https://doi.org/10.1109/PVSC.2018.8547259

do Nascimento, L.R., Braga, M., Campos, R.A., Naspolini, H.F., Rüther, R., 2020. Performance assessment of solar photovoltaic technologies under different climatic conditions in Brazil. Renew. Energy 146, 1070–1082. https://doi.org/10.1016/j.renene.2019.06.160

do Nascimento, L.R., Braga, M., Dolla, R., Campos, R.A., Ruther, R., 2018. PV Systems in Warm and Sunny Climates: Performance Assessment of Commercially Available Solar Photovoltaic Technologies under Different Climatic Conditions in the Brazilian Energy Mix, in: 2018 IEEE 7th World Conference on Photovoltaic Energy Conversion (WCPEC) (A Joint Conference of 45th IEEE PVSC, 28th PVSEC & 34th EU PVSEC). IEEE, p. 0103–0108. https://doi.org/10.1109/PVSC.2018.8547687

do Nascimento, L.R., Campos, R.A., Rüther, R., Simões, G., 2016. Avaliação de desempenho de diferentes tecnologias fotovoltaicas no nordeste brasileiro, in: VI Congresso Brasileiro de Energia Solar. p. 8.

Grammatico, M.A., Littmann, B.W., 2018. Quantifying the anti-soiling benefits of anti-reflective coatings on first solar cadmium telluride PV modules, in: IEEE 44th Photovoltaic Specialist Conference. p. 1–5. https://doi.org/10.1109/PVSC.2017.8366370

Hay, J.E., 1979. Calculation of monthly mean solar radiation for horizontal and inclined surfaces. Sol. Energy 23, 301–307. https://doi.org/10.1016/0038-092X(79)90123-3

Ineichen, P., 2011. Global irradiance on tilted and oriented planes: model validations.

Lopes, R., 2017. Energia Solar Fotovoltaica: Panorama, Oportunidades e Desafios

Mints, P., 2018. SPV Market Solar Flare Report 2018 - Issue 3.

Munshi, A.H., Sasidharan, N., Pinkayan, S., Barth, K.L., Sampath, W.S., Ongsakul, W., 2018. Thin-film CdTe photovoltaics – The technology for utility scale sustainable energy generation. Sol. Energy 173, 511–516. https://doi.org/10.1016/j.solener.2018.07.090

Passow, K., Solar, F., Francisco, S., 2018. Commercial Test of Anti-Reflective Coating on First Solar Cadmium Telluride PV Modules. 2018 IEEE 7th World Conf. Photovolt. Energy Convers. (A Jt. Conf. 45th IEEE PVSC, 28th PVSEC 34th EU PVSEC) 2709–2712.

Pereira, E.B., Martins, F.R., Abreu, S.L. de, Rüther, R., 2017. Atlas brasileiro de energia solar. 2. ed. Inpe 80. https://doi.org/978-85-17-00030-0

Perers, B., Furbo, S., Han, J., Kong, W., Stergiakis, S., 2015. Long Term Testing and Evaluation of PV Modules with and without Sunarc Antireflective Coating of the Cover Glass. Energy Procedia 70, 311–317. https://doi.org/10.1016/j.egypro.2015.02.128

Perez, R., Ineichen, P., Seals, R., Michalsky, J., Stewart, R., 1990. Modeling daylight availability and irradiance components from direct and global irradiance. Sol. Energy 44, 271–289. https://doi.org/10.1016/0038-092X(90)90055-H

PV Magazine Latin America, [s.d.]. 10,1 GW de nova energia fotovoltaica para o Brasil até 2023 [WWW Document]. URL https://www.pv-magazine-latam.com/brasil-noticias/101-gw-de-nova-energia-fotovoltaica-para-o-brasil-ate-2023/ (accessed 12.1.19).

Strevel, N., 2017. The Optimal PV Module Size.

Zomer, C. and R. Rüther, Simplified method for shading-loss analysis in BIPV systems – part 1: Theoretical study. Energy and Buildings, 2017. 141: p. 69-82.